

PROTON ACCELERATION IN AN INDUCTION LINAC\*

J. D. Ivers, John A. Nation, and I. Roth  
Laboratory of Plasma Studies and  
School of Electrical Engineering  
Cornell University  
Ithaca, New York 14853

Abstract

An account will be given of the operational characteristics of the first module of a proton induction linac. The system, which has a design output of 1.0 MeV. at 1000 A. in a 50 nsec. pulse, has a 350 keV. electrostatic accelerator for proton beam generation, followed by a 700 keV. inductively driven accelerator. The induction gap is magnetically insulated. We describe the design and performance of the accelerator and show measurements of the beam characteristics. Techniques for proton beam transport, and preliminary measurements of the beam propagation, will also be presented.

Introduction

The work described in this report represents the first phase of a study aimed at the production of kilo-ampere beams of multi-MeV. ions. Initial work will be devoted to the generation and transport of proton beams, although with some modification the same techniques may be applied to acceleration of heavier ions.

Pulse power technology advances in the last several years have now reached the point where one can generate intense ion beams at current levels of about one mega-ampere and at subohm impedance levels<sup>(1)</sup>. We are exploring in this work the use of inductive acceleration techniques for the complementary purpose of generating and transporting high energy ion beams (multi megaVolt) at current levels of a few kiloamperes. Inductive acceleration will be required for at least the final stages of any heavy ion fusion system<sup>(2)</sup> and might well also find application in the development of neutron sources.<sup>(3)</sup> The use of induction fields for acceleration is especially attractive because accelerators based on time varying magnetic fields can be stacked in series to provide a beam having a final energy equal to the sum of the output energies of the separate component accelerators. In applications requiring final beam energies of more than about ten megavolts this provides a useful technique for the production of high current beams.

Several induction accelerators have been built for the generation of electron beams. Beam parameters vary up to the 50 MeV., 20kA., design output of the ATA accelerator. The accelerators use a variety of configurations and materials<sup>(4)</sup> ranging from ferrite and iron cores on the one hand, to oil or vacuum on the other extreme. The work described here, which is aimed at the acceleration of protons, requires the addition of at least two new features, namely the provision of magnetic insulation in the accelerating gaps to suppress electron flow, and secondly the provision of electrostatic neutralization of the drifting ions to prevent the loss of the beam due to radial expansion. Both of these techniques have been developed elsewhere<sup>(5,6)</sup>. We shall only describe results obtained to date on the operation of the first megavolt of the accelerator, including the performance of the magnetic insulation of the diode. We plan to use similar

techniques to those described by Humphries<sup>(6)</sup> for the beam neutralization.

Module Design

In this section we shall describe the design used for the first megavolt of the accelerator. This design was based on the availability of a 500 kV., seven Ohm Blumlein as the pulse source. The accelerator head is shown schematically in figure 1. It is a two stage device having an electrostatically driven diode, used

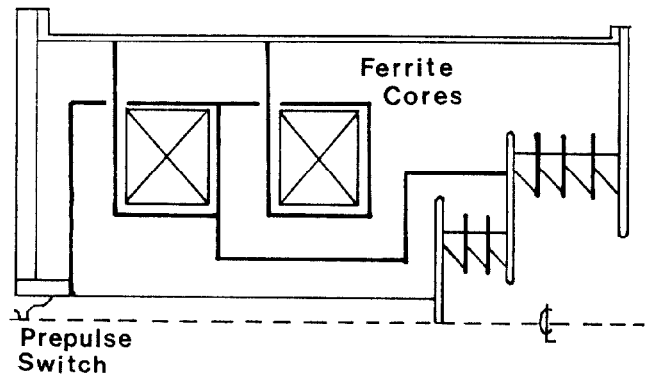


Figure 1. Simplified schematic of the accelerator module, showing both the electrostatically driven proton source and the inductive post-acceleration gap.

to generate the proton beam, followed immediately by an inductively driven section. The output of the Blumlein has a pulse duration of 50 nanoseconds so that with the 0.035 Volt-second ferrite core used one can obtain a 700 keV. acceleration in the induction gap. Since the electrostatically driven diode is directly in parallel with the ferrite cores the peak output energy of the accelerator is limited to 1.05 MeV. for a 50 nsec. pulse. The output energy has been increased above this value by driving the system harder. This is achieved, of course, at the cost of a reduction in the beam duration.

The Blumlein is separated from the load by a prepulse gap shown at the extreme left of the figure. This is essential in order that the available volt seconds of the core are not wasted during the charging cycle. The prepulse gap reduces the voltage across the load, during the charging cycle to a peak value of only a few kilovolts. This is partly due to the relatively high value of the capacitance between the primary feed and the outer shell. Each of the cores consists of seven TDK P-14 ferrite disks. The specifications of the cores are given below in Table 1:

\*Work supported by the AFOSR.

Saturation Field Strength	3.8 kG.
Remnant Magnetization	2.5 kG.
Coercive Force	0.6 Oersted
Resistivity	$>10^6 \Omega \text{ cm.}$
Outer Diameter	50.8 cm.
Inner Diameter	25.4 cm.
Core Width	2.5 cm.

Table 1. Electrical and Mechanical Specifications of the Ferrite Cores.

The two cores are in parallel as shown in the figure. Note that the figure has been simplified to illustrate the connections. In practice there are three rods providing the radial electrical connections. The rods are spaced at  $120^\circ$  to each other. The axial conductors are cylinders at present, but will later be replaced by rods to reduce the stray capacitance to the surroundings. The secondary winding follows the outer conducting shell and encloses both sets of cores. The secondary voltage appears across the front diode gap. The electrostatic diode and the induction gap both use graded lucite rings for insulation.

In parallel with the cores there is a direct connection to the back diode from the Blumlein. The ground return for this electrostatically driven gap follows the conductors shown between the center feed and the cores, i.e. the path does not enclose the ferrites.

A simple schematic, not indicating losses, is given in figure 2 of the electrical connection. In

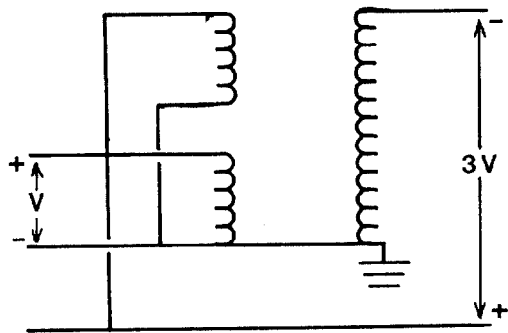


Figure 2. Electrical schematic, not showing losses, of the acceleration module.

essence the system is an autotransformer with a ground connection through to the secondary between the diode and the induction gap. This technique, which could only be used once in a multistage accelerator, has the advantage of reducing the total amount of ferrite needed for the accelerator to only two-thirds of that which would be needed if all of the acceleration were provided inductively. Similar techniques can not be used in later stages as they would require introduction of an additional system ground.

#### Diode Design

The physical arrangement of the accelerating gaps is illustrated in figure 3. The electrostatically driven gap is located in front of the insulators to allow for mounting of the magnetic field coils shown. The anode consists of a polyethylene shaped disc having an emitting area of about  $25 \text{ cm}^2$ . Metallic pins are mounted through the polyethylene and are electrically

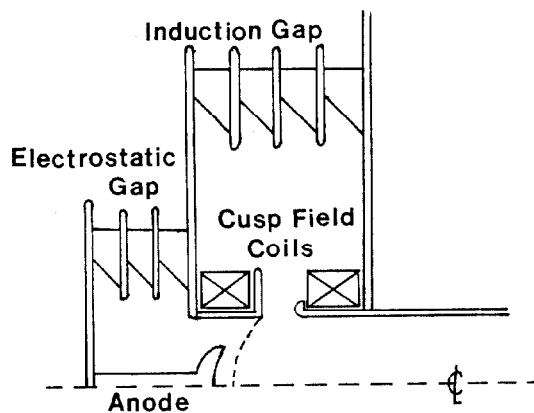


Figure 3. Acceleration gap detail, illustrating the injector, the post acceleration gap, and the magnetic insulation geometry.

connected to the anode plate. These pins serve as the source of a flashover anode plasma, which is in turn the proton source for the accelerator. Protons accelerated through the diode enter the induction gap through a transparent screen. The total proton flux is determined from activation yields, using the 470 keV.

resonance reaction  $^{12}\text{C}(p, \gamma)^{13}\text{N}$ . The diode is run presently in the bipolar flow mode, partly as a matter of convenience (and permitted by the low generator source impedance) and partly to enhance the proton flux. The magnetic fields used in the induction gap are shaped to prevent the reverse electron flow in that gap. Most of the flow occurs at radii equal to or greater than the 3.8 cm. radius of the drift tube used to transport the emergent beam. The cusp field must be sufficiently strong that the magnetron radius of the electrons emitted from the drift tube wall is less than the gap spacing. This field is computed to be about 2 kG. The field coils are mounted within the vacuum envelope of the diode to minimize effects due to the penetration time of the field lines through the metal.

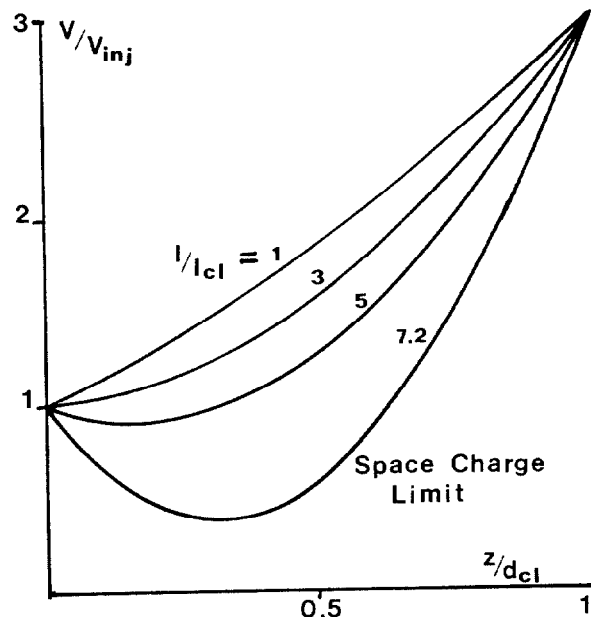


Figure 4. Results of a one-dimensional calculation illustrating the effect of a finite ion injection energy on the space charge limiting current.

In fact, we use a short rise time pulse so that the magnetic field is shaped within the gap to follow the contour of the conductors. Figure 4 shows the results of a one-dimensional computation of the potential distribution within the induction gap for the specific case corresponding to the injection energy used. The ordinate represents the beam energy normalized to the injection energy of the protons (from the diode), and the abscissa is the gap location normalized to the spacing for space charge limited proton flow for zero injection energy. The parameter beside each curve shows the proton current normalized to the corresponding zero injection energy vacuum space charge limit. The effect of the finite injection energy of the protons is to allow an increase in the permitted current density over the zero injection energy value by a factor of 7.2. Alternately the diode gap can be increased by a factor of about 2.7 over the zero injection energy space charge limited spacing and still permit flow of the injected proton current. This latter option is the one used as this provides a maximum in the gap spacing and hence a minimum in the electron current attempting to cross the induction gap.

### Experimental Results

Figure 5 shows waveforms for the Induction gap voltage and current, the electrostatic gap current and the pulse line voltage. The waveforms to the left and right of the figure show the results obtained with and

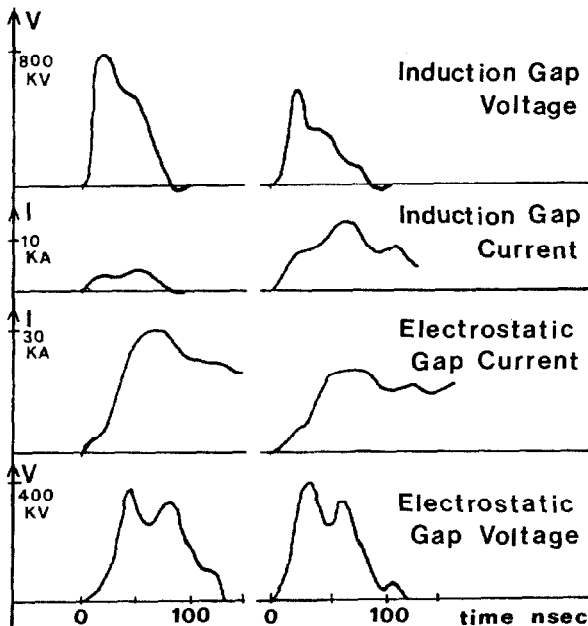


Figure 5. Comparison of beam characteristics with and without magnetic insulation. The data to the left of the figure was obtained with magnetic insulation and that to the right without insulation.

without magnetic insulation. The base pressure in the diode was  $3 \times 10^{-4}$  Torr. Operation at slightly higher pressure resulted in substantially higher diode currents. The peak induction gap current, monitored during the pulse, was about 4.0 kA, compared with the about 17 kA without the insulation. The induction gap diode voltage pulse reached a peak value of 790 kV, compared to 660 kV without the insulation. The shape of the pulse is also considerably improved by the magnetic insulation. These first results on the operation of the module are encouraging and suggest that we should be able to operate in a mode inhibiting most of the electron flow. In the particular data presented in this paper, we estimate that the proton beam current reached a peak value of approximately 250 Amperes. This figure is based on Carbon activation data to determine the total number of accelerated protons, and assumes a current waveform similar in duration and shape to the induction gap voltage pulse. The figure is also consistent with the measured bipolar mode beam current in the electrostatic gap and the known mesh transparency. Note that the reduction in the electrostatic gap current without magnetic insulation is always present and probably due to the Blumlein source impedance of seven Ohms.

### Beam Transport

We intend to study proton beam transport, including beam emittance, in drift tubes using this beam. In order to obtain propagation it will be necessary to provide a source of electrostatic neutralization for the beam. We shall attempt to provide the necessary electrons from several flashboards mounted in the tube wall. The electrons from the flashboard plasmas will be drawn into the proton beam by the space charge fields of the beam. To date we have only operated without neutralization. Rapid expansion of the proton beam was observed at rates comparable to that expected from a non neutralized beam.

### Acknowledgements

We wish to acknowledge the useful contributions made by Mr. D. Aster to the early development of this project.

### References

1. J. A. Nation. Particle Accelerators. 10, 1-30, (1979).
2. A. Faltens, E. Hoyer, D. Keefe, L. Jackson Laslett. IEEE Trans. Nucl. Sci. NS-26, 3106, 3109 (1979).
3. R. Jameson. IEEE Trans. Nucl. Sci. NS-26, 2986-2991 (1979). See also M. Foss, Proc. Heavy Ion Fusion Workshop LBL Report 10301, 68-76 (Nov. 1979).
4. D. Eccleshall and J. Temperly. J. Appl. Phys. 49, 3669 (1978).
5. P. Dreike, C. Eichenberger, S. Humphries, Jr., and R. N. Sudan. J. Appl. Phys. 47, 85, (1976).
6. S. Humphries, "Intense Pulsed Ion Beams for Fusion Applications," Sandia Report 80-0402 (April 1980).